Contribution by synaptic zinc to the gender-disparate plaque formation in human Swedish mutant APP transgenic mice

Joo-Yong Lee*, Toby B. Cole†, Richard D. Palmiter†, Sang Won Suh‡, and Jae-Young Koh*§

*National Creative Research Initiative Center for the Study of Central Nervous System Zinc and Department of Neurology, University of Ulsan College of Medicine, Seoul 138-736, Korea; †Howard Hughes Medical Institute, Department of Biochemistry, Box 357370, University of Washington, Seattle, WA 98195; and ‡Department of Anatomy and Neuroscience, University of Texas Medical Branch, 625 Jennie Sealy Hospital, Galveston, TX 77555

Edited by L. L. Iversen, University of Oxford, Oxford, United Kingdom, and approved March 15, 2002 (received for review January 21, 2002)

Endogenous metals may contribute to the accumulation of amyloid plaques in Alzheimer's disease. To specifically examine the role of synaptic zinc in the plaque accumulation, Tg2576 (also called APP2576) transgenic mice (*hAPP*$^+$) expressing cerebral amyloid plaque pathology were crossed with mice lacking zinc transporter 3 (*ZnT3*$^{-/-}$), which is required for zinc transport into synaptic vesicles. With aging, female *hAPP*$^+$:*ZnT3*$^{+/+}$ mice manifested higher levels of synaptic zinc, insoluble amyloid β, and plaques than males; these sex differences disappeared in *hAPP*$^+$:*ZnT3*$^{-/-}$ mice. Both sexes of *hAPP*$^+$:*ZnT3*$^{-/-}$ mice had markedly reduced plaque load and less insoluble amyloid β compared with *hAPP*$^+$:*ZnT3*$^{+/+}$ mice. Hence, of endogenous metals, synaptic zinc contributes predominantly to amyloid deposition in *hAPP*$^+$ mice.

Alzheimer's disease (AD) is characterized by deposition of amyloid plaques and neurofibrillary tangles in the brain (1, 2). The main component of the plaque is a 39–43-aa peptide named amyloid β peptide (Aβ), derived from a proteolytic cleavage of the β-amyloid precursor protein (APP) of 695–770 amino acids (3, 4). Under physiological conditions, Aβ aggregates to form insoluble amyloid fibrils, whose deposition may cause physiologic abnormality and neuronal cell death (2).

A growing body of evidence suggests that endogenous metal ions such as zinc, copper, or iron may contribute to aggregation of Aβ and accumulation of plaques. First, zinc or copper induces the rapid aggregation of synthetic Aβ in an aqueous environment (5, 6), likely by binding to histidine residues within Aβ (7, 8). Second, concentrations of the transition metals including zinc and copper are elevated in AD brains, more so around plaques (9–11). Finally, the treatment with metal chelators resulted in the dissolution of aggregated Aβ from AD brain extracts (12) and inhibited accumulation of amyloid plaques in human Swedish mutant APP_{695} (Tg2576, also called APP2576) transgenic mice (13).

Of endogenous metals, zinc has been found at high levels in all of the congophilic amyloid plaques of human AD brain (14) as well as Tg2576 mice (15). Whereas potential sources of zinc in plaques are diverse, histochemically reactive zinc in synaptic vesicles in particular has several interesting characteristics. First, its abundance in olfactory bulb, cerebral cortex and the limbic area, and its scarcity in cerebellum (10, 16–18) correlate with the regional distribution of plaques (19–21). For example, although the cerebellum contains widespread diffuse Aβ deposits (22), this structure lacks amyloid plaques (15, 23). Second, thus far, synaptic zinc is the only zinc that has been demonstrated to be released with neuronal activity into the extracellular space (17, 24), where Aβ mainly accumulates. Although extracellular zinc concentrations are normally low (<1 μM), at the peak of neuronal activity, they may exceed 100 μM (24), a concentration sufficient to promote aggregation of Aβ (7, 12).

Zinc transport into synaptic vesicles is coincident with the expression of zinc transporter 3 (ZnT3) and is completely abrogated in *ZnT3*-null (*ZnT3*$^{-/-}$) mice (25, 26). To explore the possibility that synaptic zinc has a disproportionately critical role for Aβ accumulation in Tg2576 transgenic (*hAPP*$^+$) mice (15, 21), we produced three mouse genotypes (*hAPP*$^+$:*ZnT3*$^{+/+}$, *hAPP*$^+$:*ZnT3*$^{+/-}$, and *hAPP*$^+$:*ZnT3*$^{-/-}$) by breeding *hAPP*$^+$ mice with the *ZnT3*$^{-/-}$ mice (26). In the present study, we demonstrate that synaptic zinc, which constitutes only 20–30% of the total zinc, contributes predominantly to gender-disparate accumulation of congophilic plaques in AD brain.

Materials and Methods

Generation of *hAPP*$^+$:*ZnT3*$^{-/-}$ Mice. Three different genotypes (*hAPP*$^+$:*ZnT3*$^{+/+}$, *hAPP*$^+$:*ZnT3*$^{+/-}$, and *hAPP*$^+$:*ZnT3*$^{-/-}$) of mice were produced by first crossing female Tg2576 transgenic *hAPP*$^{+/-}$ mice (C57BL/SJL hybrid background) with male *ZnT3*$^{-/-}$ mice (C57BL/129sv hybrid background), and then interbreeding the offspring (*hAPP*$^{+/-}$:*ZnT3*$^{+/-}$). Therefore, all mice used for the present study are of the identical strain backgrounds. Genotypes of littermates were determined by PCR, using the recommended primers both for *ZnT3* (26) and *hAPP* (27). Because homozygous *hAPP*$^{+/+}$ mice died prematurely, only hemizygous *hAPP*$^+$ mice were used for this study.

Determination of Synaptic Zinc by *N*-(6-Methoxy-8-quinolyl)-*p*-carboxybenzoylsulfonamide (TFL-Zn) Histofluorescence. We measured zinc fluorescence in hippocampi of non-Tg2576 littermates (*hAPP*$^{-/-}$), because the dense zinc fluorescence in the plaques might falsely increase the signal in presynaptic terminals. Without fixation, brain sections (10-μm thick) were stained with the zinc-specific fluorescent dye TFL-Zn (0.1 mM; Calbiochem) dissolved in Tris buffer (pH 8.0), and photographed with a digital camera (Camedia C2000; Olympus, Tokyo) linked to a fluorescence microscope (Olympus BX60; excitation, 355–375 nm; dichroic, 380 nm; barrier, 420 nm). Fluorescence intensity in the mossy fiber region of the hippocampus was measured with an image analysis program (IMAGE-PRO, Media Cybernetics, Silver Spring, MD). All values, after subtraction of background fluorescence in thalamus that lacks synaptic zinc (26), were normalized to the mean fluorescence of the corresponding area in 6-month-old, male, wild-type mice as 100%.

Measurement of Total Metal Content. Removed brains were immediately placed on ice. Left cerebral hemispheres were weighed, digested in ultrapure nitric acid, air-dried, and suspended in 2% nitric acid. Right cerebral hemispheres were quickly frozen in liquid nitrogen and stored for later Aβ analysis. Metal contents containing zinc, iron, and copper were measured

This paper was submitted directly (Track II) to the PNAS office.

Abbreviations: AD, Alzheimer's disease; APP, β-amyloid precursor protein; hAPP, human APP; Aβ, amyloid β; ZnT3, zinc transporter 3; TFL-Zn, *N*-(6-methoxy-8-quinolyl)-*p*-carboxybenzoylsulfonamide.

See commentary on page 7317.

§To whom reprint requests should be addressed. E-mail: jkko@www.amc.seoul.kr.

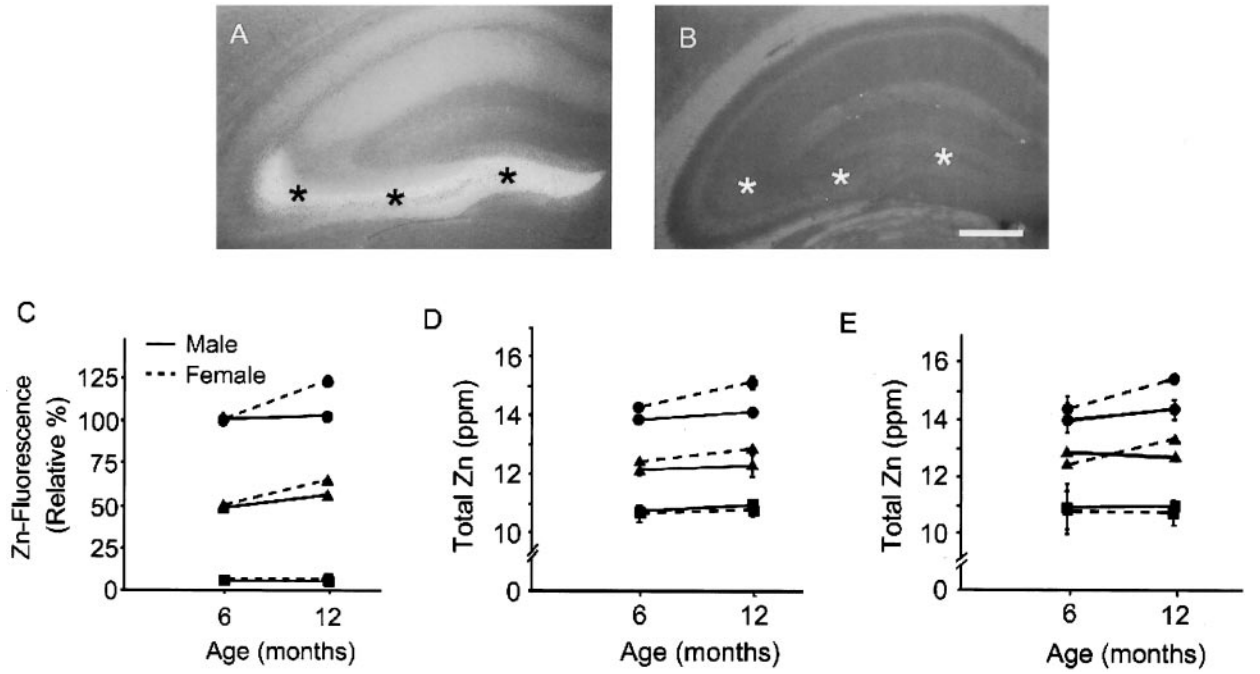

Fig. 1. Gender-disparate increases of synaptic zinc in mice with aging. (*A* and *B*) Fluorescence photomicrographs of coronal brain sections of non-Tg2576 ($hAPP^{-/-}$), $ZnT3^{+/+}$ (*A*), and $ZnT3^{-/-}$ (*B*) mice stained with TFL-Zn. Whereas dense zinc fluorescence was seen in the hippocampal mossy fiber area of $ZnT3^{+/+}$ mice (*A*, asterisks), virtually no zinc fluorescence was seen in the same area of $ZnT3^{-/-}$ mice (*B*, asterisks). (Bar = 100 μm.) (*C*) Data denote TFL-Zn fluorescence (mean ± SEM, $n = 6$) in the hippocampal mossy fiber area (asterisks in *A* and *B*) of $hAPP^{-/-}$ mice with different *ZnT3* genotypes. Differences in zinc fluorescence among $ZnT3^{+/+}$, $ZnT3^{+/-}$, and $ZnT3^{-/-}$ at 6 and 12 months were all significant ($P < 0.001$). Differences between male and female were significant only at 12 months in $ZnT3^{+/+}$ and $ZnT3^{-/-}$ ($P < 0.001$). (*D*) Total zinc content (mean ± SEM, $n = 3$) in brains of non-Tg2576 mice ($hAPP^{-/-}$) with different *ZnT3* genotypes. (*E*) Total zinc content (mean ± SEM, $n = 3$) in brains of $hAPP^{+}$ mice with different *ZnT3* genotypes. Circles, triangles, and squares denote $ZnT3^{+/+}$, $ZnT3^{+/-}$, and $ZnT3^{-/-}$, respectively.

by inductively coupled plasma atomic emission spectrophotometer (ICP-AES; model 138 Ultrace; Jobin Yvon, North London, U.K.) and expressed as parts per million of wet weight. Additionally, total zinc content in the cerebellum was also measured.

Tissue Preparation and Congo Red Staining. Brains were harvested and immediately frozen in liquid nitrogen. Coronal brain sections of 10-μm thickness were obtained with a cryostat (Leica, Nussloch, Germany) and mounted on poly-L-lysine-coated glass slides.

Plaques were identified with Congo red staining. After staining in Gill's hematoxylin solution (Sigma) for 10 min, brain sections were rinsed in tap water for 5 min, and incubated in alkaline sodium chloride solution for 20 min. Brain sections were then stained with alkaline Congo red solution (0.2% in 80% ethanol saturated with sodium chloride; Sigma) and washed in absolute ethanol.

Quantification of Congophilic Plaque Loads in the Brain. The total number of congophilic plaques was manually counted under light microscope (magnification ×400; Olympus) in 10 coronal sections taken every 650 μm from bregma + 3.0 mm. The percent area loaded with plaques was measured from the hippocampi and cerebral cortices of 15- or 18-month-old mice with an image analysis program (IMAGE-PRO).

Sandwich ELISA to Measure the Soluble or Insoluble A$\beta_{40/42}$. Levels of soluble or insoluble A$\beta_{40/42}$ in the whole brain of *hAPP*-transgenic mice were measured by the sandwich ELISA method (BioSource International, Camarillo, CA). After right cerebral hemispheres were homogenized and centrifuged in Tris·HCl buffer (20 mM, pH 7.6) containing EDTA (10 mM) and protease inhibitor mixture (Roche Diagnostics), the supernatants (soluble fraction) were taken. The pellets were resuspended and homogenized in 70% formic acid (insoluble fraction). Following the appropriate dilution, levels of soluble or insoluble A$\beta_{40/42}$ were measured by the sandwich ELISA method, using a mAb specific for the NH_2 terminus of human Aβ as capture Ab and biotinylated rabbit polyclonal Ab specific for the 1–40 or 1–42 sequence of human Aβ as detection Ab.

Statistical Analysis. All values were presented as mean ± SEM. Differences between groups were assessed by one-way ANOVA followed by post hoc Student–Newman–Keuls test. A P value less than 0.05 was considered significant.

Results

General Characteristics of $hAPP^{+}$:$ZnT3^{-/-}$ Mice. Because homozygous $hAPP^{+/+}$ mice died prematurely, we used only hemizygous $hAPP^{+}$ mice for this study. $hAPP^{+}$ mice lacking *ZnT3* exhibited no differences from wild-type mice with respect to body size, gross morphology, fertility, longevity, or behavior. Moreover, brain regions that normally have abundant synaptic zinc appear normal by light and electron microscopies (26), although there is an increased susceptibility of these mice to kainate-induced seizures (28).

Attenuation of Synaptic or Total Zinc in $hAPP^{+}$:$ZnT3^{-/-}$ Mice. Staining of brains with the zinc-specific fluorescent dye, TFL-Zn, which detects the zinc in synaptic vesicles (29, 30), showed *ZnT3* copy number-dependent decrease of fluorescence intensity in hippocampus and cerebral cortex at 6–12 months of age ($P <$ 0.001, one-way ANOVA with post hoc Student–Newman–Keuls test) (Fig. 1 *A–C*). In $ZnT3^{+/+}$ mice, dense zinc fluo-

Table 1. Levels of brain iron and copper in various groups

Genotype for *ZnT3*	Sex	Age, months	Level, ppm Fe^{2+}	Level, ppm Cu^{2+}
+/+	F	6	20.7 ± 0.22	2.4 ± 0.02
		12	22.2 ± 0.21	2.6 ± 0.05
	M	6	19.8 ± 0.14	2.2 ± 0.05
		12	21.9 ± 0.24	2.5 ± 0.03
+/−	F	6	20.9 ± 0.17	2.4 ± 0.05
		12	21.4 ± 0.24	2.6 ± 0.08
	M	6	21.4 ± 0.27	2.6 ± 0.03
		12	21.2 ± 0.08	2.4 ± 0.09
−/−	F	6	20.7 ± 0.21	2.4 ± 0.09
		12	21.1 ± 0.36	2.3 ± 0.06
	M	6	19.9 ± 0.24	2.0 ± 0.12
		12	20.7 ± 0.04	2.5 ± 0.08

All values are represented as mean ± SEM (n = 3 for each). There was no difference among groups by one-way ANOVA.

rescence was seen in the hippocampal mossy fibers (asterisks in Fig. 1*A*). In contrast, no zinc fluorescence was seen in *ZnT3*$^{-/-}$ mice, even in the normally zinc-rich mossy fibers (asterisks in Fig. 1*B*) (26). Zinc fluorescence of hippocampi increased significantly between 6 and 12 months of age in *ZnT3*$^{+/+}$ and *ZnT3*$^{+/-}$ females, but not in *ZnT3*$^{-/-}$ females and all genotypes of male (Fig. 1*C*). In contrast to zinc fluorescence, total zinc content of cerebrum of *ZnT3*$^{-/-}$ or *ZnT3*$^{+/-}$ mice was reduced by only about 30% or 15%, respectively, in both nontransgenic (Fig. 1*D*) and *hAPP*$^{+}$ mice (Fig. 1*E*). Hence, synaptic zinc may constitute about 30% of total brain zinc, which is close to the previous estimate (26). As seen with synaptic zinc above, age-related increases in total zinc were seen in a *ZnT3* copy number-dependent manner only in *ZnT3*$^{+/+}$ and *ZnT3*$^{+/-}$ female mice. In contrast, levels of iron or copper were not different among male and female *ZnT3*$^{+/+}$, *ZnT3*$^{+/-}$, and *ZnT3*$^{-/-}$ mice at two different ages (Table 1).

Diminished Plaque Load in *hAPP*$^{+}$:*ZnT3*$^{-/-}$ Mice. After 12 months of age, number and size of congophilic plaques increased markedly. Staining of hippocampal sections of 24-month-old *hAPP*$^{+}$:*ZnT3*$^{+/+}$ mice with TFL-Zn and Congo red revealed numerous congophilic plaques (Fig. 2*C*), all of which also exhibited dense zinc fluorescence (Fig. 2*A*). By contrast, *hAPP*$^{+}$:*ZnT3*$^{-/-}$ mice that lacked synaptic zinc (Fig. 2*B*) showed markedly decreased plaque load at the same age (Fig. 2*D*).

Accumulation of Aβ plaques was quantitated by counting plaques in brain sections stained with Congo red. The number of plaques at 12 months of age was substantially reduced in *hAPP*$^{+}$:*ZnT3*$^{-/-}$ mice as compared with that in *hAPP*$^{+}$:*ZnT3*$^{+/+}$ mice, with the number of plaques found in *hAPP*$^{+}$:*ZnT3*$^{+/-}$ mice falling in between (Fig. 3). In agreement with previous reports (31), there were more plaques in the brains of female *hAPP*$^{+}$:*ZnT3*$^{+/+}$ mice than in the brains of male mice. This gender difference was reduced in *hAPP*$^{+}$:*ZnT3*$^{+/-}$ mice ($P <$ 0.05) and disappeared in *hAPP*$^{+}$:*ZnT3*$^{-/-}$ mice (P = 0.535) (Fig. 3).

The number of plaques increased with age in all three genotypes; however, the increase was greatest in *ZnT3*$^{+/+}$ mice (Fig. 4*A*). The extent of plaque deposition, estimated as the percent of the area that is loaded with plaques, was greatly reduced at 15 and 18 months of age in *ZnT3*$^{-/-}$ compared with *ZnT3*$^{+/+}$ mice (Fig. 4*B*). The more conspicuous reduction of total plaque area than plaque numbers in *ZnT3*$^{-/-}$ mice is attributable to the smaller average size of plaques in *ZnT3*$^{-/-}$ mice (Fig. 5 and Table 2).

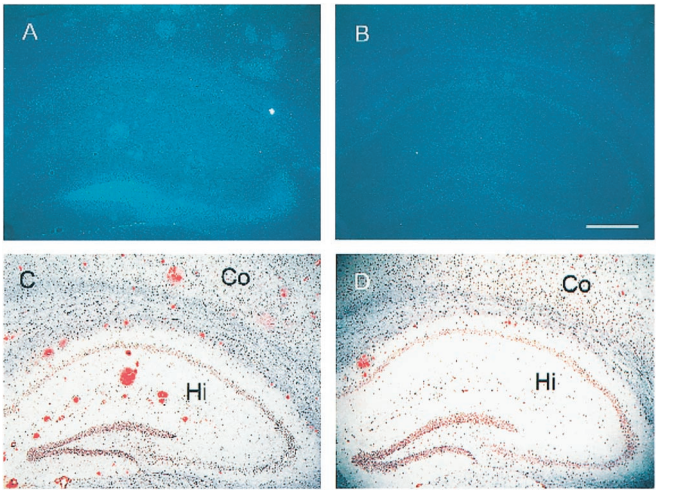

Fig. 2. Reduced deposition of amyloid plaques in *hAPP*$^{+}$:*ZnT3*$^{-/-}$ mouse brains. (*A–D*) Coronal sections of 24-month-old female *hAPP*$^{+}$ mouse brains with *ZnT3*$^{+/+}$ (*A* and *C*) or *ZnT3*$^{-/-}$ (*B* and *D*) genotype, stained with TFL-Zn (*A* and *B*) or Congo red (*C* and *D*). Compared with *ZnT3*$^{+/+}$ mice that had numerous TFL-Zn- and Congo red-stained plaques in cerebral cortex (Co) and hippocampus (Hi), *ZnT3*$^{-/-}$ mice had markedly reduced number of plaques. (Bar = 100 μm.)

It is possible that differences in background strains affect the phenotype of transgenic mice expressing *hAPP*. In fact, we have found that the *hAPP*$^{+/-}$:*ZnT3*$^{+/+}$ F1 mice had higher plaque burden than the original Tg2576 transgenic mice at 12 months of age (213.7 ± 25.7 vs.121.1 ± 17.9 plaques per 10 coronal sections, respectively). However, for data analysis, we used only F1 animals derived from crossing *hAPP*$^{+/-}$:*ZnT3*$^{+/-}$ mice with the identical strain backgrounds.

Increased Ratio of Soluble/Insoluble Aβ in *hAPP*$^{+}$:*ZnT3*$^{-/-}$ Mice. Next, we examined the effect of synaptic zinc on levels of soluble and insoluble Aβ. The levels of insoluble Aβ40 and Aβ42 were reduced substantially in *hAPP*$^{+}$:*ZnT3*$^{-/-}$ mice at 12 and 18

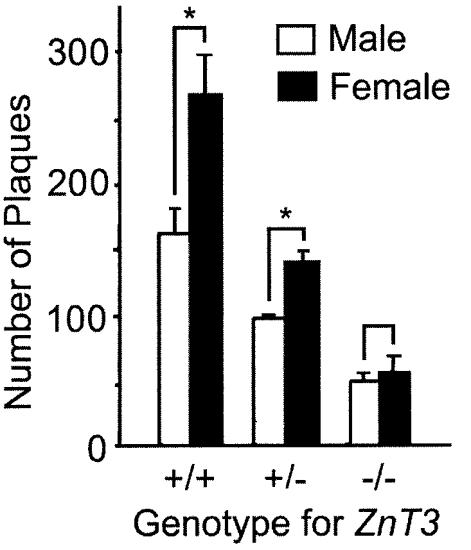

Fig. 3. The effect of synaptic zinc deficiency on gender-disparate deposition of amyloid plaques. Data denote number (mean + SEM, n = 5 each) of congophilic plaques in 10 coronal brain sections of 12-month-old male and female *hAPP*$^{+}$ mice with indicated *ZnT3* genotypes. Asterisks represent significant difference between male and female ($P < 0.05$).

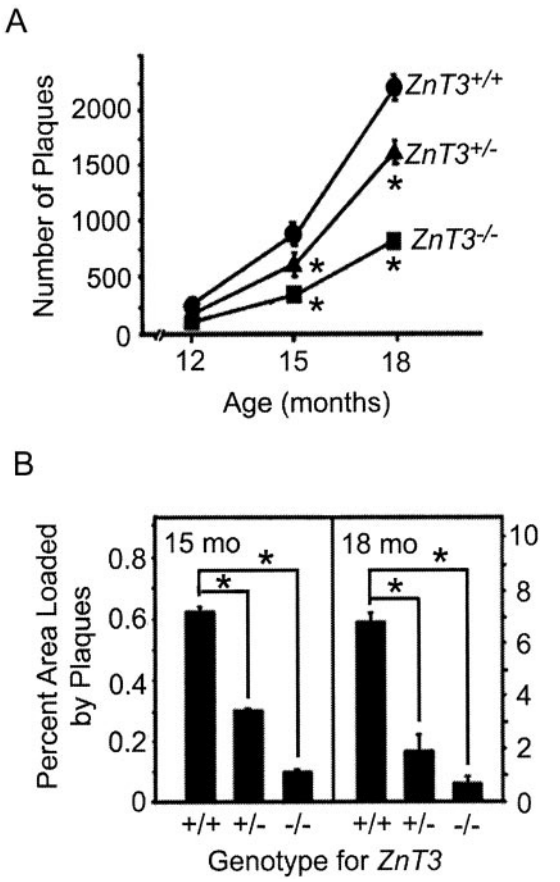

Fig. 4. Reduction of the plaque load in $ZnT3^{-/-}$ mice. (*A*) Age-dependent increases in the number of amyloid plaques (mean ± SEM, $n = 3$–5 each) in $hAPP^{+}$ female mice with indicated *ZnT3* genotypes. Asterisks denote difference from $ZnT3^{+/+}$ ($P < 0.01$). (*B*) Percent area occupied by congophilic amyloid plaques in coronal brain sections of 15- or 18-month-old female $hAPP^{+}$ mice with indicated *ZnT3* genotypes. Asterisks represent significant difference ($P < 0.05$).

months of age as compared with those in $hAPP^{+}$:$ZnT3^{+/+}$ mice (Fig. 6). Whereas the gender difference was observed in $hAPP^{+}$:$ZnT3^{+/+}$ mice only for insoluble Aβ42 at 12 months of age, at 18 months of age the gender difference became more conspicuous for both insoluble and soluble Aβ40 and Aβ42.

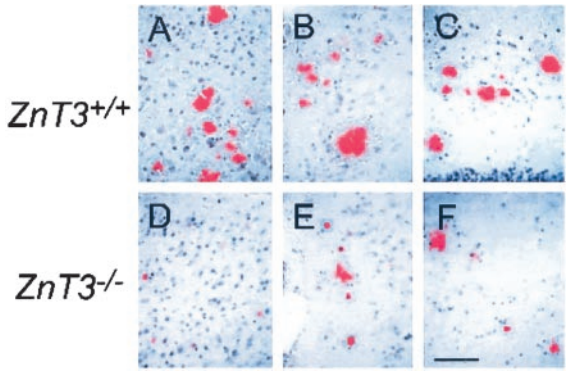

Fig. 5. Reduced plaque sizes in $hAPP^{+}$:$ZnT3^{-/-}$ mice. Photomicrographs of frontal cortex (*A* and *D*), parietal cortex (*B* and *E*), and hippocampi (*C* and *F*) of 18 month-old female $ZnT3^{+/+}$ (*A*–*C*) and $ZnT3^{-/-}$ (*D*–*F*) $hAPP^{+}$ mice stained with Congo red. Note that plaques in $ZnT3^{-/-}$ brains are much smaller than those in $ZnT3^{+/+}$ (also see Table 1). (Bar = 100 μm.)

Table 2. Variations of plaque sizes in different *ZnT3* genotypes

Genotype for *ZnT3*	+/+	+/−	−/−
Maximum, μm²	8,020	4,520	1,410
Minimum, μm²	11.01	2.14	0.56
Mean ± SEM, μm² ($n = 5$)	572 ± 34.3	259 ± 13.6*	188 ± 7.1**

* and ** denote differences from $ZnT3^{+/+}$ mice at $P < 0.005$ and $P < 0.001$, respectively (one-way ANOVA followed by post hoc Student–Newman–Keuls test).

Interestingly, changes in the levels of soluble Aβ40 and Aβ42 were just the opposite of those of insoluble Aβ; $hAPP^{+}$:$ZnT3^{-/-}$ mice had more soluble Aβ than $hAPP^{+}$:$ZnT3^{+/+}$ mice. As results, at 18 months of age, $ZnT3^{-/-}$ mice showed much higher soluble/insoluble ratios of Aβ40 and Aβ42 (1.3–1.5) as com-

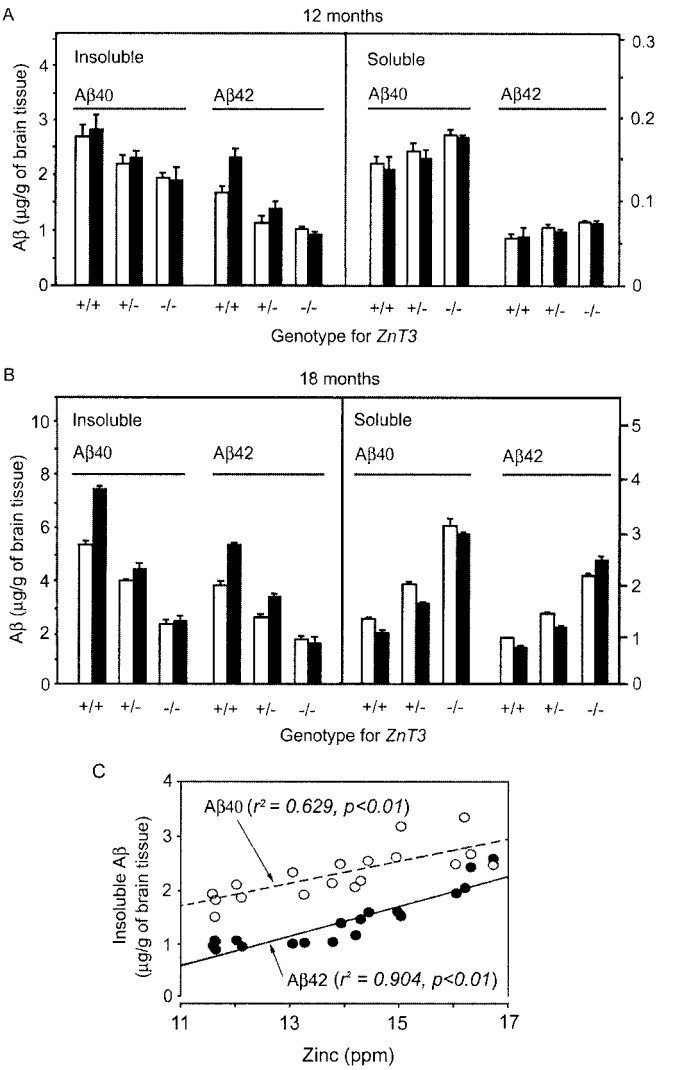

Fig. 6. The absence of synaptic zinc alters levels of soluble and insoluble Aβ. (*A*) Bars denote concentrations of insoluble and soluble Aβ40 and Aβ42 (μg/g of brain tissue; mean + SEM, $n = 3$ each) in 12-month-old male (empty bars) and female (filled bars) $hAPP^{+}$ mice with indicated *ZnT3* genotypes. (*B*) Concentrations of insoluble and soluble Aβ40 and Aβ42 (μg/g of brain tissue) in 18-month-old male (empty bars) and female (filled bars) $hAPP^{+}$ mice with indicated *ZnT3* genotypes ($n = 2$). (*C*) Correlations between levels of insoluble Aβ42/Aβ40 and total zinc. Regression analysis showed positive correlations in both cases ($P < 0.01$).

pared with $ZnT3^{+/+}$ mice (0.1–0.3). Interestingly, whereas the levels of insoluble Aβ in $hAPP^{+}$:$ZnT3^{+/+}$ mice were greater in female, the levels of soluble Aβ tended to be greater in male. These gender differences disappeared in $hAPP^{+}$:$ZnT3^{-/-}$ mice. Finally, we examined correlations between levels of insoluble Aβ and total zinc at 12 months of age (Fig. 6*C*). Levels of total zinc were positively correlated with levels of insoluble Aβ42 and Aβ40 (both $P < 0.01$) (Fig. 6*C*). On the other hand, there were inverse correlations between total zinc and soluble Aβ40 and Aβ42 levels ($P < 0.05$, not shown).

Discussion

Evidences obtained *in vitro* suggest that zinc may contribute to Aβ aggregation and thus plaque formation (5–8). The recent demonstration that metal chelation ameliorates Aβ plaque formation in $hAPP^{+}$ mice strongly supports this hypothesis (13). However, sources of zinc in the plaques have not been known. Our results have demonstrated that, specifically, zinc in synaptic vesicles, which is under the control of ZnT3 (25, 26), plays a major role in Aβ formation.

Synaptic zinc in the forebrain is stored in the vesicles as glutamatergic terminals and is released into the extracellular environment during normal neuronal activity (17, 24, 32). During periods of intense neuronal activity, e.g., during seizures, extracellular zinc concentrations can rise dramatically. Although zinc uptake transporters undoubtedly recycle zinc that is released into the synaptic cleft, the released zinc could contribute to Aβ aggregation and plaque formation. This releasable pool of zinc represents about 20–30% of total zinc in regions where ZnT3 is expressed (Fig. 1) (26). Because the absence of synaptic zinc by deleting *ZnT3* in Tg2576 mice markedly reduced the plaque load and increased the ratio of soluble/insoluble Aβ, it is likely that synaptic zinc plays a disproportionately larger role in shifting the equilibrium toward the Aβ aggregation and plaque accumulation.

It is well known that the age-adjusted incidence for AD is substantially higher in females than males (33). Consistently, the plaque load in Tg2576 mice showed the same intersexual disparity (31). Although causes for this are unknown, our studies suggest that female-restricted increases of synaptic vesicle zinc may play a crucial role in the sexually disparate accumulation of amyloid plaques in Tg2576 mice. The increase in synaptic zinc with aging exclusively in female correlated well with higher levels of insoluble Aβ and plaque loads in female. These gender differences completely disappeared in $ZnT3^{-/-}$ mice, further suggesting the role for synaptic zinc in these gender differences. It would be intriguing to see whether levels of ZnT3 are under the control of sex hormones.

That some small plaques still form in $ZnT3^{-/-}$ mice may be attributable to the requirement for zinc of numerous diverse functions in the brain and elsewhere. This finding is little surprising because every cell contains a large number of zinc-binding proteins (34, 35). Thus, it is likely that to meet metabolic requirements for zinc in the brain, a significant amount of zinc may come in and out of the brain. Some of such dynamic zinc, although normally less in amounts than synaptic zinc, may bind in the extracellular space to Aβ and transform it to insoluble forms. These residual pools of zinc, as well as copper and iron, may contribute to basal Aβ deposition in *ZnT3*-null mice (5, 6, 36). Alternatively, neuronal death or neurite degeneration around Aβ deposition may release zinc from breakdown of zinc-binding proteins.

Currently, diverse strategies to prevent AD or reverse its pathology are under consideration. Of these, the main efforts are directed toward the idea that Aβ accumulation is the central pathogenic event (37). The β- and γ-secretases are the main targets for the development of drugs to reduce the generation of Aβ (38, 39). Abs against Aβ also seem promising for reducing or even preventing the plaque load (40–42). Our results support the idea that zinc chelation therapy (13), which preferentially reduces insoluble forms of Aβ, may be an alternative therapeutic strategy to slow or prevent the onset of AD.

We thank Dr. Karen Hsiao (University of Minnesota) for generously donating the Tg2576 mice. This study was supported by Creative Research Initiatives of the Korean Ministry of Science and Technology (J.Y.K.) and National Institutes of Health grant DK-53013 (to R.D.P.).

1. Price, D. L. & Sisoda, S. S. (1998) *Annu. Rev. Neurosci.* **21,** 479–505.
2. Selkoe, D. J. (1999) *Nature (London)* **399,** A23–A31.
3. Masters, C. L., Simms, G., Weinman, N. A., Multhaup, G., McDonald, B. L. & Beyreuther, K. (1985) *Proc. Natl. Acad. Sci. USA* **82,** 4245–4249.
4. Kang, J., Lemaire, H. G., Unterbeck, A., Salbaum, J. M., Masters, C. L., Grzeschik, K. H., Multhaup, G., Beyreuther, K. & Muller-Hill, B. (1987) *Nature (London)* **325,** 733–736.
5. Bush, A. I., Pettingell, W. H., Multhaup, G., de Paradis, M., Vonsattel, J. P., Gusella, J. F., Beyreuther, K., Masters, C. L. & Tanzi, R. E. (1994) *Science* **265,** 1464–1467.
6. Miura, T., Suzuki, K., Kohata, N. & Takeuchi, H. (2000) *Biochemistry* **39,** 7024–7031.
7. Huang, X., Atwood, C. S., Moir, R. D., Hartshorn, M. A., Vonsattel, J. P., Tanzi, R. E. & Bush, A. I. (1997) *J. Biol. Chem.* **272,** 26464–26470.
8. Yang, D. S., McLaurin, J., Qin, K., Westaway, D. & Fraser, P. E. (2000) *Eur. J. Biochem.* **267,** 6692–6698.
9. Deibel, M. A., Ehmann, W. D. & Markesbery, W. R. (1996) *J. Neurol. Sci.* **143,** 137–142.
10. Danscher, G., Jensen, K. B., Frederickson, C. J., Kemp, K., Andreasen, A., Juhl, S., Stoltenberg, M. & Ravid, R. (1997) *J. Neurosci. Methods* **76,** 53–59.
11. Lovell, M. A., Robertson, J. D., Teesdale, W. J., Campbell, J. L. & Markesbery, W. R. (1998) *J. Neurol. Sci.* **158,** 47–52.
12. Cherny, R. A., Legg, J. T., McLean, C. A., Fairlie, D. P., Huang, X., Atwood, C. S., Beyreuther, K., Tanzi, R. E., Masters, C. L. & Bush, A. I. (1999) *J. Biol. Chem.* **274,** 23223–23228.
13. Cherny, R. A., Atwood, C. S., Xilinas, M. E., Gray, D. N., Jones, W. D., McLean, C. A., Barnham, K. J., Volitakis, I., Fraser, F. W., Kim, Y. *et al.* (2001) *Neuron* **30,** 665–676.
14. Suh, S. W., Jensen, K. B., Jensen, M. S., Silva, D. S., Kesslak, P. J., Danscher, G. & Frederickson, C. J. (2000) *Brain Res.* **852,** 274–278.
15. Lee, J. Y., Mook-Jung, I. & Koh, J. Y. (1999) *J. Neurosci.* **19,** RC10 (1–5).
16. Perez-Clausell, J. (1996) *J. Chem. Neuroanat.* **11,** 99–111.
17. Frederickson, C. J., Suh, S. W., Silva, D., Frederickson, C. J. & Thompson, R. B. (2000) *J. Nutr.* **130,** 1471S–1483S.
18. Jo, S. M., Won, M. H., Cole, T. B., Jensen, M. S., Palmiter, R. D. & Danscher, G. (2000) *Brain Res.* **865,** 227–236.
19. Games, D., Adams, D., Alessandrini, R., Barbour, R., Berthelette, P., Blackwell, C., Carr, T., Clemens, J., Donaldson, T., Gillespie, F., *et al.* (1995) *Nature (London)* **373,** 523–527.
20. Zhan, S. S., Veerhuis, R., Kamphorst, W. & Eikelenboom, P. (1995) *Neurodegeneration* **4,** 291–297.
21. Hsiao, K., Chapman, P., Nilsen, S., Eckman, C., Harigaya, Y., Younkin, S., Yang, F. & Cole, G. (1996) *Science* **274,** 99–102.
22. Joachim, C. L., Morris, J. H. & Selkoe, D. J. (1989) *Am. J. Pathol.* **135,** 309–319.
23. Styren, S. D., Kamboh, M. I. & DeKosky, S. T. (1998) *J. Comp. Neurol.* **396,** 511–520.
24. Assaf, S. Y. & Chung, S. H. (1984) *Nature (London)* **308,** 734–736.
25. Wenzel, H. J., Cole, T. B., Born, D. E., Schwartzkroin, P. A. & Palmiter, R. D. (1997) *Proc. Natl. Acad. Sci. USA* **94,** 12676–12681.
26. Cole, T. B., Wenzel, H. J., Kafer, K. E., Schwartzkroin, P. A. & Palmiter, R. D. (1999) *Proc. Natl. Acad. Sci. USA* **96,** 1716–1721.
27. Hsiao, K. K., Borchelt, D. R., Olson, K., Johannsdottir, R., Kitt, C., Yunis, W., Xu, S., Eckman, C., Younkin, S. & Price, D. (1995) *Neuron* **15,** 1203–1218.
28. Cole, T. B., Robbins, C. A., Wenzel, H. J., Schwartzkroin, P. A. & Palmiter, R. D. (2000) *Epilepsy Res.* **39,** 153–169.
29. Budde, T., Minta, A., White, J. A. & Kay, A. R. (1997) *Neuroscience* **79,** 347–358.
30. Lee, J. Y., Cole, T. B., Palmiter, R. D. & Koh, J. Y. (2000) *J. Neurosci.* **20,** RC79 (1–5).
31. Callahan, M. J., Lipinski, W. J., Bian, F., Durham, R. A., Pack, A. & Walker, L. C. (2001) *Am. J. Pathol.* **158,** 1173–1177.
32. Howell, G. A., Welch, M. G. & Frederickson, C. J. (1984) *Nature (London)* **308,** 736–738.

33. Katzman, R., Aronson, M., Fuld, P., Kawas, C., Brown, T., Morgenstern, H., Frishman, W., Gidez, L., Eder, H. & Ooi, W. L. (1989) *Ann. Neurol.* **25,** 317–324.
34. Vallee, B. L., Coleman, J. E. & Auld, D. S. (1991) *Proc. Natl. Acad. Sci. USA* **88,** 999–1003.
35. Vallee, B. L. & Falchuk, K. H. (1993) *Physiol. Rev.* **73,** 79–118.
36. Atwood, C. S., Moir, R. D., Huang, X., Scarpa, R. C., Bacarra, N. M. E., Romano, D. M., Hartshorn, M. A., Tanzi, R. E. & Bush, A. I. (1998) *J. Biol. Chem.* **273,** 12817–12826.
37. Soto, C. (1999) *Mol. Med. Today* **5,** 343–350.
38. Vassar, R. & Citron, M. (2000) *Neuron* **27,** 419–422.
39. Walter, J., Kaether, C., Steiner, H. & Haass, C. (2001) *Curr. Opin. Neurobiol.* **11,** 585–590.
40. Schenk. D. Barbour, R., Dunn, W., Gordon, G., Grajeda, H., Guido, T., Hu, K., Huang, J., Johnson-Wood, K., Khan, K., *et al.* (1999) *Nature (London)* **400,** 173–177.
41. Janus, C., Pearson, J., McLaurin, J., Mathews, P. M., Jiang, Y., Schmidt, S. D., Chishti, M. A., Horne, P., Heslin, D., French, J., *et al.* (2000) *Nature (London)* **408,** 979–982.
42. Morgan, D., Diamond, D. M., Gottschall, P. E., Ugen, K. E., Dickey, C., Hardy, J., Duff, K., Jantzen, P., DiCarlo, G., Wilcock, D., *et al.* (2000) *Nature (London)* **408,** 982–985.